THE UNKNOWN (UN) PART OF FUN REVEALED. Tezer M. Esat*, R.H. Spear* and S.R. Taylor+, Dept. of Nuclear Physics, Research School of Physical Sciences*, and Research School of Earth Sciences+, Australian National University, Canberra, Australia.

Following our discovery[1] of pervasive isotopic fractionation effects in Mg in a subset of Allende inclusions characterized by a highly fractionated (Group II) REE pattern we have concentrated our efforts on elucidating the nature of the small but distinct excesses in δ^{26}Mg in the same samples. Our earlier results combined with previous work[2] on FUN samples can be summarized as follows:

(a) there is a direct correlation between the highly fractionated REE patterns of Group II inclusions and Mg isotopic fractionation $\Delta(^{25}Mg/^{24}Mg)$;

(b) the fine-grained Group II aggregates have negative values of $\Delta(^{25}Mg/^{24}Mg)$ corresponding to an enrichment of the lighter Mg isotopes;

(c) in contrast coarse-grained inclusions have positive values of $\Delta(^{25}Mg/^{24}Mg)$ corresponding to an excess in the heavier Mg isotopes;

(d) all of the Group II inclusions that we have studied exhibit non-uniform isotopic fractionation;

(e) -ve/+ve non-linear effects in δ^{26}Mg are correlated with +ve/-ve fractionation in coarse-/fine-grained inclusions;

(f) all of the above points, so far as they have been investigated, apply to Si isotopes as well[3]. The symmetries between the coarse- and fine-grained inclusions are such that there must be a strong generic relationship between them. The most puzzling attribute is the excesses or deficits in δ^{26}Mg. Deficits in Mg rich phases in coarse-grained inclusions can be related to solar system material that did not receive its full complement of ^{26}Al. Similarly the excesses in fine-grained inclusions could be due to ^{26}Al decay in phases with relatively high abundance of ^{27}Al. The alternative explanation associates the anomalies in δ^{26}Mg to an artefact of a non-linear fractionation process. Thus, in one case the cause would be due to nuclear processes and in the other due to unspecified physiochemical effects. In order to differentiate between the two possibilities we have undertaken laboratory experiments in an attempt to induce isotopic fractionation in Mg. Pyroxene crystals separated from a sample of eclogite from Yakutia were subjected to distillation. Each sample, weighing about 50 mg, was placed in a carbon boat and heated with an RF induction coil in a bell jar in vacuum ($\approx 5\times10^{-5}$ torr). After melting, the samples coalesced into small spheres and began to visibly vaporize at about 2150°C. Part of the vaporized material was collected on teflon disks placed ≈8cm above the carbon boat. Seven samples were subjected to distillation for varying periods of time ranging up to 1/2 hr and the sample weight was recorded before and after. The evaporation residues and the condensates were then dissolved in a mixture of HF + HNO_3 acids and small aliquots were directly loaded for Mg isotopic analysis in the ANU 61cm multi-cup mass spectrometer. The results are summarized in Table 1 and Figs. 1 and 2. The data in Table 1 show:

(a) significant isotopic fractionation can be induced in the laboratory by distillation;

(b) the evaporation residues are enriched in the heavy Mg isotopes and the evaporation condensates in the light Mg isotopes;

(c) distillation induces non-linear offsets in δ^{26}Mg that are not accounted for by the simple fractionation laws used to fit the data. The linear law was used in the present case. Other similarly formulated recipes also fail to account for the observed offsets;

(d) the non-linear effects, +ve/-ve δ^{26}/Mg are correlated with -ve/+ve mass fractionation in an identical fashion to those observed in the Allende fine-/coarse-grained inclusions.

In Fig. 1 we compare the induced fractionation in the evaporation residues to that predicted by the Rayleigh law. The initial and final amounts of ^{25}Mg were assumed to be proportional to the initial and final weights of the samples. The unshaded ellipses represent the entries in Table 1. The spread of each point along the y-axis is typical of the uncertainties in $\Delta(^{25}Mg/^{24}Mg)$. The experimental points roughly follow the trend of the Rayleigh distillation curve. For comparison, we also show the expected mass loss from the fractionated Allende inclusions C-1, EK-1-4-1, EGG-3 and 4691 (dark ellipses). The variation of the magnitude of the non-linear effects $|\delta^{26}|$ with the magnitude of the induced fractionation are shown in Fig. 2 for evaporation residues and condensates (unshaded/dark ellipses). The condensates appear to exhibit larger non-linear effects than residues for a given magnitude of fractionation. Although there is a rough linear trend for both sets, there is no precise correlation with fractionation. In a closed system, consideration of mass-balance requires that the isotopic effects in the residue should mirror the effects in the condensate. The large differences in the data both for fractionation and δ^{26}Mg between the two sets shows that, in the present experiment, condensation was selective and heterogenous. Presumably, the environment in the solar nebula approximates an open system rather than a closed one. The labelled points represent fractionated Allende inclusions with established +ve or -ve non-linear effects. Inclusion EK-1-4-1 appears to be

© Lunar and Planetary Institute • Provided by the NASA Astrophysics Data System

significantly displaced from the general trend exhibited by most of the data. The non-linear effects we have been able to generate so far are small <3‰. Nevertheless, it is clear that the observed negative δ^{26}Mg in fractionated coarse-grained Allende FUN inclusions is a direct result of kinetic fractionation processes. The interpretation of the positive δ^{26}Mg in the fine-grained FREE FUN[1] inclusions is complicated by the possible presence of ^{26}Al. However, it is most likely that the observed positive offsets in inclusions 3529-40, 3529-43 and 5242 are wholly due to kinetic effects and not to ^{26}Al, as they lie within the field defined by the present data. The largest mass loss recorded during the present experiments was less than 60%. The condensed material (+ve δ^{26}/Mg) was sampled during the whole of the distillation process. It is possible that differential sampling by omitting the earlier stages of distillation could produce much larger effects. Furthermore, it may be possible to generate large ^{26}Mg excesses with only a small apparent linear isotopic fractionation. Back-reaction of such material into pre-existing coarse-grained inclusions containing melilite and anorthite with subsequent partial recrystallization could mimic the behaviour expected from ^{26}Al decay in high ^{27}Al phases. In this regard, we note that the rim materials enclosing coarse-grained inclusions are mineralogically similar to the constituents of fine-grained inclusions[4]. Perhaps, a more pertinent translation for the acronym FUN would be Fractionation and Unknown Nebular anomalies. In the following paper we enumerate the implications of the present findings for Mg as well as for other elements and the constraints it places on the early history of the meteoritic materials and the solar nebula.

[1] Esat & Taylor, LPSC XV (1984) 252-255;
[2] Wasserburg & Papanastassiou, in Essays in Nucl. Astr. Camb. Univ. Press (1981);
[3] Molini-Velsko, Mayeda & Clayton, LPSC XIV (1983) 509;
[4] Wark & Lovering, LPSC VIII (1977) 95.

Table 1. Fractionation and non-linear effects in Mg isotopes. Pyroxene crystals from a sample of eclogite from Yakutia were subjected to distillation at a mean temperature of 2150°C in vacuum (~5×10^{-5} torr). Initial weight of each sample was about 50 mg[c]. Mg isotopic composition of unprocessed pyroxenes is normal.

	Sample	Mass Loss %	Fractionation [a] $\Delta(^{25}Mg/^{24}Mg)$‰. amu^{-1}	δ^{26}Mg [b] ‰
#1	Condensate	3.8	- 1.4	+0.38±0.16
#2	Residue	23	+ 3.3	-0.02±0.07
	Condensate		-12.2	+2.34±0.12
#3	Residue	42.6	+ 8.7	-0.68±0.06
	Condensate		- 6.9	+1.65±0.08
#4	Residue	59	+27	-1.05±0.08
	Condensate		- 1.4	+0.74±0.05
#5	Residue	32.7	+ 3.8	+0.23±0.06
	Condensate		-13.6	+1.88±0.06
CL	Condensate	-	- 6.1	+1.07±0.08
BG	Residue	51	+18.1	-0.48±0.16

[a] $\Delta(^{25}Mg/^{24}Mg)=[(^{25}Mg/^{24}Mg)_{meas}/(^{25}Mg/^{24}Mg)_{GM}-1]\times10^3$; where GM is the grand mean value 0.12386 determined from repeat analyses of normals. Reproducibility for repeat runs is better than ±1.5‰.

[b] Excess ^{26}Mg following normalization to remove fractionation: the quoted errors are $2\sigma_{mean}$.

[c] EPMA analyses yield SiO_2 36.5, Al_2O_3 10.7, MgO 12.5, CaO 40.3 for evaporation residue BG; and SiO_2 54.5, Al_2O_3 2.9, Cr_2O_3 1, FeO 1.2, MgO 16.5, CaO 23.4, Na_2O 0.5 for the unprocessed samples (wt.%).

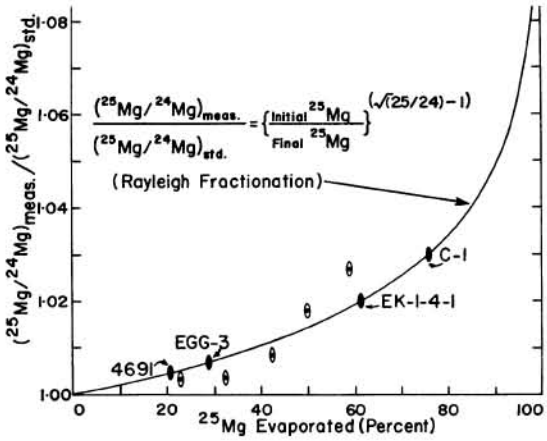

Fig 1. Isotopic mass fractionation in evaporation residues (unshaded ellipses) compared with the predictions of the Rayleigh law. FUN inclusions C-1, EK-1-4-1, EGG-3 and 4691 have been plotted on the Rayleigh curve to indicate the corresponding mass-loss.

Fig 2. The variation in the magnitude of non-linear offsets in δ^{26}Mg with the degree of isotopic mass fractionation. Open/shaded ellipses correspond to residues (enriched in heavy Mg)/condensates (enriched in light Mg) respectively. The labelled points represent Allende inclusions with established non-linear effects.

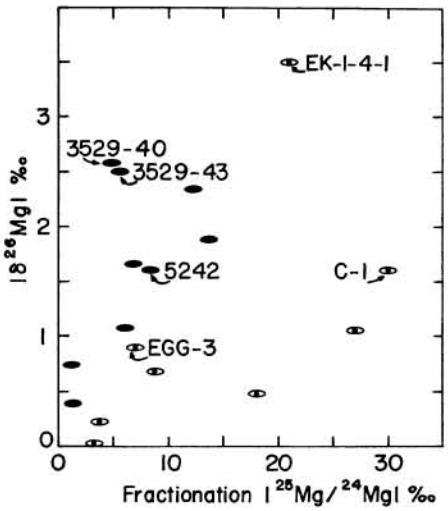

© Lunar and Planetary Institute • Provided by the NASA Astrophysics Data System